Synthesis and Characterization of Polydentate Schiff-Base Ligands and Their Complexes

Havva Demirelli,[1] Mehmet Tümer,[*2] and Ayşegül Gölcü[2]

[1]Department of Chemistry, Faculty of Education, Gazi University, 06100, Ankara, Turkey

[2]Department of Chemistry, Faculty of Science and Arts, K.Maraş Sütçü İmam University, 46100, K.Maras, Turkey

Received May 31, 2005; E-mail: mtumer@ksu.edu.tr

In this study, we synthesized the amine compounds 2-{(E)-[(2-aminoethyl)imino]methyl}phenol (H_3A) and 2-{(E)-[(3-aminopropyl)imino]methyl}-6-methoxyphenol (H_3B) as the starting materials. From reactions of the starting materials with 2-hydroxy-5-methylisophthalaldehyde, phthalaldehyde, and 2-hydroxy-5-t-butylisophthalaldehyde, we prepared the new ligands H_3L^1–H_3L^3 and H_2L. The Cu(II) and Cd(II) complexes of the ligands have been obtained. Microanalytical data, magnetic moment, $^1H(^{13}C)$ NMR, mass spectra, FT-IR, and conductivity measurements have been used to explain the structures of the ligands and their complexes. The protonation constants of the ligands H_3L^1–H_3L^3 have been studied in a 1:1 molar ratio (M:L). Protonation and stability constants of the Schiff bases and their Cu(II) and Cd(II) complexes have been determined by the potentiometric titration method in 50% dioxane–water media at $25.00 \pm 0.02\,°C$ under a nitrogen atmosphere and ionic strength of 0.1 M $NaClO_4$. The ligands H_3L^1–H_3L^3 have seven protonation constants. In other words, the ligand H_2L has six protonation constants. The variation of protonation constants of these compounds were interpreted on the basis of structural effects exposed by the substituents.

Since proton transfer is known to be crucial for physico-chemical properties and practical application of Schiff bases, this process has been widely studied in the literature.[1,2] It has been shown that the position of the tautomeric equilibrium depends not only on the electronic structure of the molecule, but also on its conformation. The interactions between the non-bonded atoms in molecules, leading to the strengthening of the hydrogen bond, as well as the intramolecular interactions in the solid state, stabilizing the planar structure of the molecule, shift the equilibrium toward the NH form.[3] The intramolecular proton-transfer reaction proceeds comparatively easily in the *ortho*-hydroxy Schiff bases. Intramolecular π-electron coupling leads to the strengthening of the hydrogen bonds in these systems. These compounds are potential materials for molecular memory and optical switch devices[4] or fluorescent probes of biological systems.[5]

Among the different physicochemical properties of organic compounds, protonation and stability constants determined in mixed solvents provide an important basis for speculation about whether substituent effects influence their acidic and basic properties. It is also accepted that knowledge of the stability constants of such Schiff bases and their metal complexes may eventually help to throw some light on the inactivation of essential trace metals in biological systems. Therefore, it was interesting to determine the protonation and stability constants of some Schiff bases–metal complexes in dioxane–water media of different compositions potentiometrically.[6] The study of the complex formation of Schiff bases can not be carried out in aqueous solution because the ligands H_3L^1–H_3L^3 and their Cu(II) and Cd(II) complexes are not soluble in water media. A dioxane–water mixture is a typical binary solution, as the dielectric constant can be varied from 2.2 to 78 at 25 °C. Another interesting characteristic of this system is that non-polar dioxane is completely miscible with water at every ratio. The dioxane–water mixture (50:50%) has been chosen as the solvent mixture for our study. In such a medium, the Schiff bases and metal complexes are soluble giving stable solutions.

Numerous electrochemical studies have been made for a fairly large number of acyclic and macrocyclic Cu(II) complexes derived from Schiff bases. These investigations revealed that the redox properties of the Cu(II) complexes are markedly influenced by structural and electronic factors.[7,8]

The present study deals with the synthesis, characterization, and electrochemical and potentiometric determination of the Schiff bases and their metal complexes. In addition, we study the stability constants of their Cu(II) and Cd(II) complexes by the potentiometric titration method in 50:50% dioxane–water media at $25.00 \pm 0.02\,°C$ and an ionic strength of 0.10 M $NaClO_4$. The obtained data from titrations were evaluated by the computer program BEST.[9]

Experimental

Materials. Stock solutions of the Schiff bases were prepared in purified dioxane.[10] Doubly distilled conductivity (Millipore system) water was used as the aqueous medium as well as for the preparation of dioxane–water mixtures. All the other chemicals used were of A.R. grade and were used without further purification. Stock solutions of 0.03 M $Cu(ClO_4)_2$ and $Cd(ClO_4)_2$ were standardized using the appropriate indicator by EDTA titrations.[11] Sodium hydroxide solutions were prepared as 50% (v/v) aqueous dioxane solutions. The concentration of NaOH and absence of carbonate were frequently checked by means of Gran plots[12] using potassium hydrogen phthalate (Merck) as the acid. The acid solutions (0.1 M) prepared from Merck pa perchloric acid were titrated

against a standardized 0.1 M sodium hydroxide solution.[13] The ionic strength of each solution was adjusted to 0.10 M by the addition of NaClO$_4$ as the supporting electrolyte. All organic and inorganic materials with solvents were purchased from Fluka or Merck. 2-Hydroxy-5-methylisophthalaldehyde and 2-hydroxy-5-*t*-butylisophthalaldehyde were obtained according to the literature method.[14] Physical measurements and ^{1}H(^{13}C) NMR data of the ligands and their Cd(II) complexes have been given in the Supporting Information.

Potentiometric Apparatus and Procedure. Potentiometric titrations were carried out in jacketed glass reaction vessels as described in Ref. 9. The cell EMF was measured using an Orion EA 940 pH meter (resolution 0.1 mV, accuracy 0.2 μL) equipped with a Mettler Toledo Inlab 412 combined glass electrode and an Orion 960 automatic titrator containing carbonate-free sodium hydroxide at a known (≈0.1 M) concentration at 25.00 ± 0.02 °C with an ionic strength of 0.10 M (NaClO$_4$). The electrode was modified by replacing its aqueous KCl solution with 0.01 M NaCl + 0.09 M NaClO$_4$ saturated with AgCl. The temperature was maintained constant inside the cell at 25.00 ± 0.02 °C by water circulation from a Haake thermostatted bath (precision ± 0.02). All potentiometric measurements were carried out in water–dioxane mixtures containing 50% dioxane (v/v) because of the low solubility of the Schiff bases and possible hydrolysis in aqueous solutions. Potentiometric titrations were carried out at constant temperature and in an inert atmosphere of nitrogen with CO$_2$-free standardized 0.1 M NaOH in a 50.0 mL solution containing 0.1 M NaClO$_4$ (i) 2.5×10^{-3} M HClO$_4$ (for cell calibration), (ii) 6.0×10^{-3} M HClO$_4$ + 1.5×10^{-3} M Schiff base (for protonation constant of Schiff base), and (iii) 6.0×10^{-3} M HClO$_4$ + 1.5×10^{-3} M Schiff base + 1.5×10^{-3} M Cu(ClO$_4$)$_2$/Cd(ClO$_4$)$_2$ (for stability constant of Schiff base–metal complex).

Cell Calibration. The potentiometric cell was calibrated for use of the combined pH electrode as a hydrogen ion concentration probe rather than as an activity probe. The ionic strength of the test solutions used in this study was kept constant; therefore, the EMF of the cell can be written in the form

$$E_{\text{cell}} = E^{\circ'}_{\text{cell}} + E_{\text{j}} + k \log[\text{H}^+], \tag{1}$$

where $E^{\circ'}_{\text{cell}}$ represents a quantity independent of [H$^+$], but dependent on the activity of Cl$^-$ in the filling solution of the electrode and the activity coefficient of H$^+$ in the test solution.[15] The activity coefficient of H$^+$ can be considered to be constant throughout the titration because the ionic strength of the solution is almost constant. E_{j} is the liquid junction potential and the constant k, denoted as electrode calibration slope, represents the Nernst factor. The calibration constants $E^{\circ'}_{\text{cell}}$ and k, were determined by titration with a 2.5×10^{-3} M solution of HClO$_4$ and 0.1 M NaOH solution for the reaction media. All the solutions for the calibration titrations were made up to an ionic strength of 0.1 M NaClO$_4$. In all titrations, the experimental points in the region $2.2 < \text{pH} < 3.0$ were used for calibrations, where pH represents $-\log[\text{H}^+]$. Within this range of pH, the E_{j} is effectively constant.[15] Equation 1 in the form $E_{\text{cell}} = +E^{\circ}_{\text{cell}} + k \log[\text{H}^+]$, where $E^{\circ}_{\text{cell}} = E^{\circ'}_{\text{cell}} + E_{\text{j}}$, was found to reproduce the calibration data to a precision typically of the order of ± 1.0 mV. The standardization of the combined pH electrode was checked in the alkali range too by the addition of an excess of NaOH. By assuming the E°_{cell} value determined in the acidic range to be reliable and [OH$^-$] = concentration of base added in excess, we calculated reproducible values of pK_{w}, for the solvent mixtures examined[16,17] and obtained the pK_{w} value of 15.37 in this media.

Treatment of Potentiometric Data. The ligand protonation and metal ion stability constants were calculated with the FORTRAN program BEST[9] and were obtained through the algebraic solution of the mass and charge balance equations evaluated at each equilibrium point of the formation curves. The input for the program BEST consists of the components, the concentrations of each component and initial estimates of the equilibrium constant for each species. The species considered present in the experimental solutions were those that one would expect to form according to the principles of coordination chemistry. The program refines stability constants by the iterative nonlinear least-squares fit of potentiometric equilibrium curves through a set of simultaneous mass balance equations for all the components expressed in terms of known and unknown equilibrium constants. By suitable use of the program, it is possible to obtain a high degree of discrimination in the selection of chemical species. Multinuclear metal complexes and other species, such as ML$_n$, M$_n$L$_n$, H$_n$ML$_n$, and so on, included at various stages of refinement were rejected on the basis of increased σ values. The inclusion of these species did not improve the estimated standard deviation and the value of their equilibrium constants progressively decreased without convergence. The best set of complexes was: ML, HML, H$_2$ML, H$_3$ML, and H$_4$ML for Cu(II); ML, HML, H$_2$ML, H$_3$ML, H$_4$ML, and H$_5$ML for Cd(II). All the models converged at $\sigma < 0.02$p[H] units of the observed p[H] values, which is considered to be an acceptable fit. The equilibrium constants reported in this paper were obtained as averaged values of three titrations. Species distribution curves were calculated with the FORTRAN program SPE.[9]

Synthesis of the Starting Materials H$_3$A and H$_3$B. The precursors were prepared according to the modified method described earlier[18,19] by mono condensation of the appropriate diamines with aldehydes. To the vigorously stirred and cool dilute solution ($T = 5$–10 °C) of the diamine (ethylenediamine and/or 1,3-diaminopropane, 20 mmol) in absolute ethanol (100 mL), was added dropwise a cooled solution of salicylaldehyde and/or vanilline (15 mmol) in absolute ethanol (80 mL). After the addition was complete, the mixture was stirred for 15–30 min and then refluxed for 15–60 min. The resulting solution was evaporated under vacuum to remove the solvent, and excess diamine was extracted by benzene. The obtained compounds were used for the next step without further purification.

H$_3$A: Yield (40%), color: yellow, mp 105 °C. Found (% calcd): C, 65.80 (65.83); H, 7.40 (7.37); N, 17.10 (17.06). UV–vis (λ_{max}/nm, EtOH as solvent): 407, 342, 315, 290, 268, 255. IR (KBr, cm^{-1}): 3377 [ν(OH)], 2872 [ν(CH$_2$)], 2640 [ν(OH···N)], 1633 [ν(CH=N)], 1377 [ν(C–OH)]. ^{1}H NMR: (CDCl$_3$ as solvent, δ in ppm): 10.5 (s, OH), 8.68 (CH=N), 7.99–6.66 (Ar-H, m), 4.52 (t, NH$_2$), 3.23 and 3.22 (t, CH$_2$, t, CH$_2$).

H$_3$B: Yield (37%), color: dark yellow, mp 58 °C. Found (% calcd): C, 63.47 (63.44); H, 7.70 (7.74); N, 13.48 (13.45). UV–vis (λ_{max}/nm, EtOH as solvent): 419, 342, 326, 320, 302, 297, 245. IR (KBr, cm^{-1}): 3355 [ν(OH)], 2931 [ν(CH$_3$)], 2847 [ν(CH$_2$)], 2662 [ν(O–H···N)], 1632 [ν(CH=N)], 1327 [ν(C–OH)]. ^{1}H NMR: (CDCl$_3$ as solvent, δ in ppm): 10.6 (s, OH), 8.40 (CH=N), 7.60–6.18 (Ar-H, m), 4.03 (t, NH$_2$), 3.96 (OCH$_3$), 3.33 and 3.20 (t, CH$_2$). ^{13}C NMR (δ in ppm): 162.15 (CH=N), 155.20–110.15 (Ar-C), 60.47 (OCH$_3$), 20.85–20.60 (–CH$_2$–).

Synthesis of the Schiff Bases H$_3$L^1–H$_3$L^3 and H$_2$L. The unsymmetrical Schiff bases were obtained by condensation of the half units and the appropriate aldehydes. To the stirred solution of the precursor (half units, H$_3$A and H$_3$B) in absolute ethanol was added a solution of 2-hydroxy-5-methylisophthalaldehyde, 2-hy-

Table 1. Analytical and Physical Data for the Schiff-Base Ligands and Their Cu(II) and Cd(II) Complexes

| Compound | Color | Yield | mp | Found (calcd)/% | | | | |
		/%	/°C	C	H	N	Cl	Cu
H_3L^1	light brown	85	115	71.09 (71.05)	6.18 (6.20)	12.31 (12.27)	—	—
$[Cu_2(L^1)]Cl$	brown	72	>250	52.68 (52.63)	4.10 (4.06)	9.12 (9.09)	5.82 (5.77)	20.70 (20.64)
$[Cd_2(L^1)]Cl$	brown	65	>250	45.47 (45.42)	3.56 (3.51)	7.89 (7.85)	5.04 (4.98)	31.58 (31.52)
H_3L^2	yellow	80	97	68.42 (68.38)	6.67 (6.62)	10.32 (10.29)	—	—
$[Cu_2(L^2)]Cl$	black	71	>250	55.73 (55.68)	4.97 (4.94)	8.44 (8.38)	5.37 (5.31)	19.10 (19.02)
$[Cd_2(L^2)]Cl$	brown	68	>250	48.61 (48.58)	4.35 (4.31)	7.36 (7.31)	4.70 (4.64)	29.43 (29.36)
H_3L^3	light brown	87	74	69.65 (69.62)	7.23 (7.17)	9.60 (9.56)	—	—
$[Cu_2(L^3)]Cl$	black	69	215	54.77 (54.72)	5.27 (5.23)	7.54 (7.51)	4.80 (4.76)	17.11 (17.04)
$[Cd_2(L^3)]Cl$	brown	66	>250	48.42 (48.38)	4.66 (4.62)	6.67 (6.64)	4.27 (4.21)	26.73 (26.66)
H_2L	red-orange	90	72-74	73.29 (73.26)	6.15 (6.10)	13.18 (13.15)	—	—
$[Cu(H_2L)]Cl_2$	black	73	154	55.71 (55.69)	4.69 (4.64)	10.03 (9.99)	12.71 (12.66)	11.41 (11.34)
$[Cd(H_2L)]Cl_2$	orange	70	>250	51.25 (51.22)	4.22 (4.27)	9.15 (9.19)	11.70 (11.65)	18.52 (18.45)

droxy-5-*t*-butylisophthalaldehyde, or phthalaldehyde in absolute ethanol. The mixture was concentrated in vacuum by evaporation of the solvent until a colored solid precipitated. The product was collected by filtration, washed with cold ethanol, and recrystallized from the appropriate solvents (ethanol for H_2L, methanol/hexane mixture (1:1) for H_3L^1–H_3L^3) to give colored crystals.

Electronic Absorption Spectral Data in Different Solvents of the Schiff Bases H_3L^1–H_3L^3 and H_2L. **H_3L^1:** (λ_{max}/nm), hexane: 362, 322, 298, 249; toluene: 476, 364, 350, 324; dioxane–water: 426, 317, 275; MeOH: 407, 365, 315, 286, 280, 253. **H_3L^2:** (λ_{max}/nm), hexane: 363, 324, 318, 256; toluene: 438, 367, 362, 324; dioxane–water: 429, 403, 362, 322, 278; MeOH: 424, 362, 318, 280, 254. **H_3L^3:** (λ_{max}/nm), hexane: 360, 349, 336, 273, 222; toluene: 460, 366, 341, 325, 322, 286; dioxane–water: 423, 288; MeOH: 428, 395, 349, 334, 297, 288. **H_2L:** (λ_{max}/nm), hexane: 389, 350, 334, 274, 259; toluene: 462, 450, 395, 350, 334, 286; dioxane–water: 346, 336, 301, 276; MeOH: 410, 349, 332, 295, 277.

Preparation of the Complexes. The complexes were prepared by similar methods. A solution of the metal salt (M: $CuCl_2 \cdot 2H_2O$ and $CdCl_2 \cdot H_2O$) (2 mmol) in absolute EtOH (25 mL) was added to a solution of the ligands (2 mmol for the ligands H_3L^1–H_3L^3 and 1 mmol for the ligand H_2L) in absolute EtOH (20 mL) and the mixture was boiled under reflux for 6–7 h. At the end of the reaction, determined by TLC, the precipitate was filtered off, washed with EtOH and Et_2O, and dried in vacuo.

Results and Discussion

The analytical data of the compounds together with physical properties are summarized in Table 1. The data obtained from the analytical and spectroscopic analyses correspond well with the general formula $[M_2(L^n)]Cl$ [*n*: 1, 2, or 3; M: Cu or Cd] for the ligands H_3L^1–H_3L^3 and $[ML]Cl_2$ for the ligand H_2L. First, we prepared the starting materials 2-(2-aminoethyl)iminomethylphenol (H_3A) and 2-(3-aminopropyl)iminomethyl-6-methoxyphenol (H_3B) (Fig. 1). One of the major difficulties in preparing the starting materials H_3A and H_3B is due to the formation of the bis product. The other problem is very low yield. Therefore, the reaction conditions must be well adjusted. In addition, they are not stable for a long time at room temperature, and gradually decompose to the oxidized products. Therefore, these starting materials were used immediately without further purification. The ligands H_3L^1–H_3L^3 and
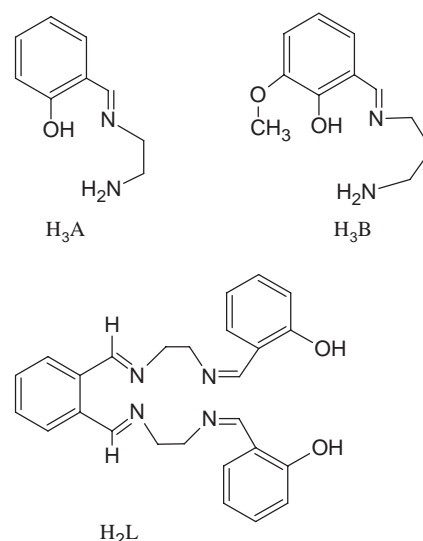

Fig. 1. General formulae of the starting materials and Schiff-base ligand H_2L.

H_2L have been synthesized from the reaction of the carbonyl and amine compounds; they are more stable than the starting compounds at room temperature. As the ligands have a lot of polar groups, such as –OH and –CH=N, they are soluble in polar organic solvents such as, EtOH, MeOH, $CHCl_3$, $(C_2H_5)_2O$, etc. It is well known that the oxygen atoms of metal complexes of salen-type ligands have anionic character, which sometimes enhances coordination strength to other metal ions.[20] We investigated the synthesis of transition-metal complexes of the ligands and prepared more soluble salen-type ligands as a host molecule by introducing hydrophobic groups such as methyl or *t*-butyl groups into the benzene rings of the ligands H_3L^1–H_3L^3.

We studied the keto–enol tautomeric forms of the ligands in the polar and non-polar organic solvents. The most useful techniques to investigate the tautomeric forms (Fig. 2) of these ligands are UV–vis and NMR spectroscopy, while IR seems of limited value here because the location of the $\nu(C=O)$ and $\nu(C-O)$ stretches in the spectra is obscured by the abundance of aromatic skeletal modes. In order to investigate the keto–enol tautomeric forms of the free ligands, the UV–vis spectra

of the same series of compounds were investigated in five solvents (hexane, methanol, ethanol, toluene, and dioxane–water (50%) mixture). The stronger solute/solvent hydrogen bonding by the hydroxy or azomethine groups, as well as the increasing importance of the solvent polarity/polarizability in the stabilization of the electronic excited state, lead to a hypsochromic shift with both increasing solvent hydrogen-bond acceptor basicity and solvent polarity/polarizability. This suggests that most of the solvatochromism in the ligands is due to the solvent polarity and basicity rather than to the solvent acidity. As the number of CH_2 groups in ROH increases, the dielectric constant decreases. If the molecules contain a polar component (OH) and a non-polar component (R), then the polarity of a compound reflects the balance between these two components. As the relative amount of hydrocarbon character increases, the polarity decreases. Note that hexane, which is 100% hydrocar-

bon, is the least polar solvent. The UV spectral data of the ligands are given in the experimental section. For example, in hexane and toluene, the ligand H_3L^1 shows eight bands in the 476–249 nm range. However, in ethanol and methanol, ligand H_3L^1 has bands in the 429–276 nm range. In non-polar solvents, the bands observed in the 476–322 nm range may be assigned to the ketoamine tautomeric form.[21] Since, in this media, there are no interactions between the ligands and solvent molecules, the ligands prefer the keto-form. However, in polar solvents, the polar groups of the ligands interact with the polar edge of the solvent and, therefore, the hydrogen bonding forms among the ligands and solvent molecules. The ligands prefer the enolimine tautomeric forms. In the toluene and hexane solvents, the free ligands have the ketoamine form. However, in dioxane–water and MeOH solvents, the enolimine forms have been observed.[22] Other ligands have similar electronic transitions in polar and non-polar organic solvents.

Electronic spectral data of the Schiff-base ligands and their Cd(II) and Cu(II) complexes in an EtOH solution are given in Table 2. The absoption spectra of the ligands are characterized by several absorption bands in the region 249–461 nm, which may be assigned to π–π^*, n–π^*, and charge-transfer transition, the longer wavelength bands are assigned to intramolecular charge transfer while the others due to π–π^* and n–π^* transition within the C=N and C–O (double character) bonds are influenced by charge-transfer interaction. All the complexes show an intense band in the 324–303 nm range, which is assigned to a π–π^* transition associated with the azomethine linkage.[23] The spectra of the complexes show intense bands in the high-energy region in the 487–358 nm range, which can be assigned to charge transfer L $\rightarrow$ M bands.[24] In the spectra of the Cu(II) complexes, the bands observed in the 628–549 nm region can be attributed to d–d transitions of the metal ions. These values are of particular importance since they were highly dependent on the geometry of the molecule. It is known that the transitions from a square-planar structure to a deformed tetrahedral structure leads to a red shift of absorption in the electronic spectra.[25] Thus, the smaller value of the wavelength of the band corresponding to the transitions resembles the geometry of the complex and that of a square-planar complex.

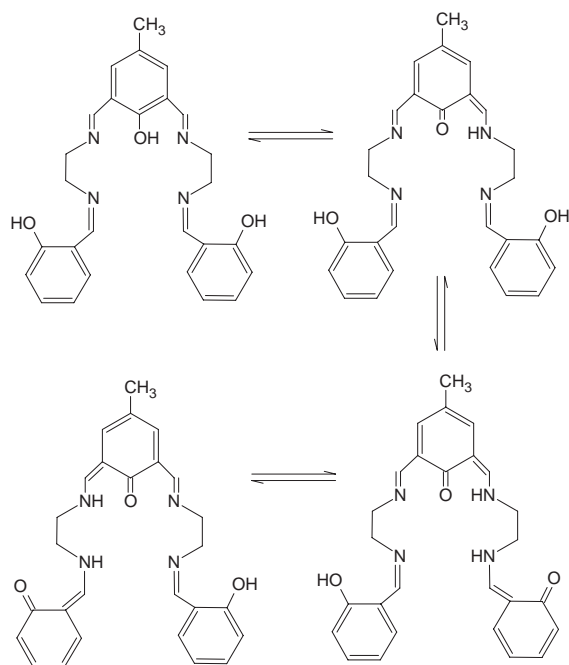IR data of the ligands and their complexes are given in

Fig. 2. Keto–enol tautomeric forms of the Schiff-base ligand H_3L^1.

Table 2. The Electronic Data of the Ligands and Their Complexes

Compound	μ_{eff} (BM)	d $\rightarrow$ d	λ_{max}/nm (ε/M^{-1} cm^{-1})			$\Lambda^{a)}$
			Charge-transfer transitions	n $\rightarrow$ π^*	$\pi \rightarrow \pi^*$	
H_3L^1	—	—	461 (1093), 411 (1137)	350 (1214), 319 (1896)	258 (1720), 52 (1559)	2.5
H_3L^2	—	—	431 (1131), 414 (893)	349 (1099), 309 (1347)	274 (1588), 285 (1462), 253 (1754)	2.3
H_3L^3	—	—	428 (1321), 412 (1066)	334 (1089)	296 (1590), 249 (1718)	1.9
H_2L	—	—	419 (887), 398 (1285)	350 (1078), 332 (1155)	296 (1634), 279 (1327),	2.8
$[Cd_2(L^1)]Cl$	Diamag.	—	361 (1259)	281 (1433)	221 (1577)	25.4
$[Cd_2(L^2)]Cl$	Diamag.	—	383 (1021)	286 (1528)	256 (1831)	27.1
$[Cd_2(L^3)]Cl$	Diamag.	—	443 (1102), 361 (1391)	325 (1285), 285 (1773)	278 (1690)	26.8
$[Cd(H_2L)]Cl_2$	Diamag.	—	422 (1052)	358 (1252)	263 (1677)	57.7
$[Cu_2(L^1)]Cl$	1.10	612 (378), 581 (299)	361 (1195)	281 (1488)	221 (1533)	30.5
$[Cu_2(L^2)]Cl$	1.11	562 (307), 549 (334)	359 (1097)	281 (1387)	220 (1584)	29.7
$[Cu_2(L^3)]Cl$	1.08	628 (417)	373 (983)	303 (1398)	281 (1587)	32.2
$[Cu(H_2L)]Cl_2$	1.71	613 (403)	377 (1123)	284 (1507)	250 (1788)	61.3

a) Λ: Ω^{-1} cm^2 mol^{-1}.

Table 3. Infrared Spectral Data[a)] for the Schiff-Base Ligands and Their Metal Complexes (cm^{-1})

Compound	ν(OH)	ν(CH$_3$)	ν(αCH$_2$)	ν(α'CH$_2$)	ν(O–H⋯N)	ν(CH=N)[b)]	ν(CH=N)[c)]	ν(M–O)	ν(M–N)
H$_3$L^1	3422 br	2945 s	2899 s	2862 s	2741 m	1634 s	1605 m	—	—
H$_3$L^2	3420 br	2959 s	2901 s	2868 s	2590 m	1633 s	1612 m	—	—
H$_3$L^3	3408 br	2953 s	2906 s	2860 s	2592 m	1632 s	1605 m	—	—
H$_2$L	3370 br	—	2901 s	2835 s	2590 m	1631 s	1620 m	—	—
[Cd$_2$(L^1)]Cl	—	2948 s	2904 s	2865 s	—	1610 s	1590 w	532 w	434 w
[Cd$_2$(L^2)]Cl	—	2952 s	2905 s	2874 s	—	1605 m	1605 w	563 w	428 w
[Cd$_2$(L^3)]Cl	—	2957 s	2909 s	2868 s	—	1610 m	1590 s	509 w	455 w
[Cd(H$_2$L)]Cl$_2$	3372 br	—	2904 s	2842 s	—	1614 s	1597 w	532 w	434 w
[Cu$_2$(L^1)]Cl	—	2947 s	2897 s	2863 s	—	1620 s	1595 s	503 w	444 w
[Cu$_2$(L^2)]Cl	—	2955 s	2898 s	2866 s	—	1613 s	1604 w	562 w	444 w
[Cu$_2$(L^3)]Cl	—	2951 s	2897 s	2865 s	—	1617 s	1600 w	534 w	448 w
[Cu(H$_2$L)]Cl$_2$	3370 br	—	2900 s	2864 s	—	1618 s	1600 w	534 w	442 w

a) br (broad), s (strong), m (medium), w (weak). b) and c) Salicylidene and diformyl fragments, respectively.

Table 3. In the spectra of the starting compounds H$_3$A and H$_3$B with the final compounds H$_3$L^1–H$_3$L^3 and H$_2$L, the broad bands in the 3370–3422 cm^{-1} range can be attributed to the ν(OH) cm^{-1} vibration. In the Cd(II) and Cu(II) complexes (except the complexes of the ligand H$_2$L), the bands due to the OH modes are no longer observed, denoting that all the hydroxy protons are displaced by Cd(II) and Cu(II) ions, leading to covalent ν(M–O) bonding with the ligands. In the ligands, the broad bands in the range 2741–2590 cm^{-1} come from the intramolecular hydrogen bonding along the phenolic –OH and azomethine –CH=N– groups; these bands disappear as complexation proceeds between the oxygen and nitrogen atoms with metals ions. The ν(CH=N) band (1634–1605 cm^{-1}) is shifted to lower wavenumbers denoting that the nitrogen atom of the azomethine group coordinates to the Cd(II) and Cu(II) ions. Because the H$_2$L ligand occurs as mononuclear complexes, the O–H group of the *o*-vanillin fragment does not coordinate to the metal ions; in the complexes of this ligand, the ν(OH) vibration is shown at 3372 and 3370 cm^{-1} for the Cd(II) and Cu(II) complexes, respectively. The bonding of the Cd(II) and Cu(II) ions to the ligands through the nitrogen and oxygen atoms is further supported by the presence of new bands in the 563–503 and 455–428 cm^{-1} range due to ν(M–O) and ν(M–N), respectively.

The molar conductivity data of all compounds in EtOH ($\approx 10^{-3}$ M solutions) are given in Table 2. The conductivity data of the Schiff-base ligands are very low and they can be regarded as non-electrolytes.[26] Moreover, all complexes have cationic form and their conductivity data are quite high (in the range 25.4–61.3 Ω^{-1} cm^2 mol^{-1}); it may be suggested that they are weak electrolytes.

The magnetic moments (as BM) of the complexes were measured at room temperature and the data are given in Table 2. The Cd(II) complexes of the ligands H$_3$L^1–H$_3$L^3 and H$_2$L are found in diamagnetic character and tetrahedral geometry around the metal ion. The structures of the mono- and binuclear Cu(II) complexes are supported by the magnetic moment data. The measured magnetic moment value of the Cu(II) complex of the ligand H$_2$L is 1.71 BM, which is very close to that of the spin only value (1.73 BM) expected for a complex having one copper(II) ion with a single unpaired electron located in an essentially $d_{x^2-y^2}$ orbital. This value suggests that the copper atom is in a tetrahedral environment in its che-

lates.[27,28] The observed magnetic moment values of the binuclear Cu(II) complexes of the ligands H$_3$L^1–H$_3$L^3 lie in the range from 1.08 to 1.11 BM. This confirms the presence of anti-ferromagnetic interaction between the two copper(II) ions. Binuclear Cu(II) complexes have a square-planar structure around the central metal ions.

The formulation of the ligands are deduced from analytical data, ^{1}H and ^{13}C NMR, and further supported by mass spectroscopy. The relatively low intensities of the molecular ion peaks, [M]$^+$, are indicative of the ease of fragmentation of the compounds, and this may reflect the number of heteroatoms present in each structure. The spectra of the ligands H$_2$L and H$_3$L^1–H$_3$L^3 show peaks at *m/e* 427, 455, 497, and 585, respectively. These peaks can be attributed to the molecular ion peaks [M]$^+$. All the ligands decompose in a similar way. In the mass spectra of the ligands, the highest intensity peaks are at *m/e* 130 (100%), 160 (100%), and 202 (100%), and may be assigned to the [C$_8$H$_6$N$_2$O]$^{2+}$, [C$_9$H$_8$N$_2$O]$^{2+}$, and [C$_{12}$H$_{14}$N$_2$O]$^{2+}$ ions, respectively, which are formed by the loss of other parts (salicylidene moiety together with diamine fragment) of the molecular ions.

The ^{1}H and ^{13}C NMR spectra of the ligands were recorded in CDCl$_3$ and the data associated with this method are given in the Supplementary Data section. All the ligands have two different surroundings. These are the 2-hydroxy-5-methyl- or -5-*t*-butylisophthalaldehyde, phthalaldehyde, and salicylidene moiety. The chemical shifts of these are different. In all ligands, there are two azomethine groups in the different centers. In addition, there are also methylene and propylene chains as bridges. In the methylene chain, there are two CH$_2$ groups. In other words, in the propylene chain, there are three CH$_2$ groups. These are shown in the different regions. The ligands show approximately the same peaks. For example, in the ^{1}H NMR spectrum of the ligand H$_3$L^1, the triplets in the 3.26–3.18 ppm range can be attributed to the protons of the CH$_2$ groups. The protons of the methyl group of the aromatic ring are observed at 2.29 ppm as a singlet. The multiplets in the 6.62–7.33 ppm range may be assigned to the protons of benzene rings. The azomethine protons of the ligand are observed in the 8.36 and 8.42 ppm range as a singlet. A singlet at 10.45 ppm may be attributed to the OH proton. When D$_2$O is added to the solution of the ligands, the OH peaks disappear. Other ligands also show similar spectral properties. In the spectrum

Table 4. Successive Protonation Constants of H_3L^1, H_3L^2, and H_3L^3 Schiff Bases in 50% Dioxane–Water Mixture ($\mu = 0.100$ M NaClO$_4$, 25.00 ± 0.02 °C)

Compound	Log K_1^H	Log K_2^H	Log K_3^H	Log K_4^H	Log K_5^H	Log K_6^H	Log K_7^H	Log β^H
H_3L^1	11.21 ± 0.02	10.78 ± 0.02	9.56 ± 0.02	8.20 ± 0.02	6.99 ± 0.02	5.23 ± 0.02	3.08 ± 0.02	55.05
H_3L^2	11.20 ± 0.02	10.75 ± 0.02	10.03 ± 0.02	8.20 ± 0.02	6.98 ± 0.02	5.30 ± 0.02	3.15 ± 0.02	55.61
H_3L^3	11.18 ± 0.02	10.70 ± 0.02	9.51 ± 0.02	8.18 ± 0.02	6.95 ± 0.02	5.25 ± 0.02	3.11 ± 0.02	54.88

of the Cd(II) complex of the H_3L^1 ligand, signals due to the hydrogen atom of the azomethine groups of the ligand shifted downfield according to the free ligand. This shows that the nitrogen atom of the azomethine group coordinates to the metal ions. The OH signals observed for the ligands disappear and this situation confirms that the phenolic C–OH group coordinates to the transition-metal ions. In the complex, the signals of the methylene groups also shifted downfield.

^{13}C NMR spectra of the ligands and their Cd(II) complexes were recorded in CDCl$_3$ and are a good diagnostic tool for determining the mode of bonding. The ^{13}C NMR spectra of the ligands and their complexes demonstrate similar properties. In the spectrum of the ligand H_3L^1, signals due to the azomethine carbon atoms are observed at 168.48 and 163.05 ppm. In the Cd(II) complex, these signals are shifted downfield, suggesting the involvement of the nitrogen lone pair in coordination with the metal ion. The signals of the carbon atoms of the benzene rings are observed approximately in the 118.95–157.75 ppm range and the signals observed in the 61.79–62.50 ppm range may be attributed to the carbon atoms of the CH$_2$ groups. The signal at 21.65 ppm can be attributed to the methyl carbon atom of the benzene ring. However, in the spectra of the Cd(II) complex, the signals due to these groups are observed at 60.05, 62.21, and 21.12 ppm. It may be suggested that these groups are not affected by complexation.

Protonation Constants of Schiff Bases.   Table 4 gives the stoichiometric protonation constants for the Schiff bases H_3L^1–H_3L^3 in a 50% dioxane–water mixture (v/v) at 25 ± 0.02 °C. The chemical structures of the Schiff bases are shown in Fig. 3 without any information about the protonation regions. As it can also be seen from Fig. 3, there are Log K_1^H, Log K_2^H, and Log K_3^H values. They show the phenolic oxygen atoms numbered with (1), (2), and (3). In addition, there are Log K_4^H, Log K_5^H, Log K_6^H, and Log K_7^H belonging to the numbers (4), (5), (6), and (7), showing the nitrogen atoms. The protonation regions of the phenolic oxygens in the Schiff bases H_3L^2 and H_3L^3 are different from the Schiff base H_3L^1. This situation may be due to the resemblance of the chemical structure of the ligands H_3L^2 and H_3L^3. Moreover, there are methoxy groups on these ligands. The methoxy groups on the Schiff-base ligands H_3L^3 and H_3L^2 are more electron-offering, and the π-electron density of the methoxy groups can delocalize on the aromatic ring with resonance.

When the structures of the Schiff bases are examined, the phenolic oxygens with numbers (2) and (3) (in the ligand H_3L^1), with numbers (1) and (2) phenolic oxygens (in the ligands H_3L^2 and H_3L^3), the imine nitrogens with numbers (4) and (5) (in the ligand H_3L^1), and the numbers (6) and (7) (in the ligands H_3L^2 and H_3L^3) imine nitrogens are identical. Martell et al. obtained similar protonation regions in their study dealing with macrocyclic ligands like our ligands.[29,30] In fact, the identical protonation regions are supposed to have
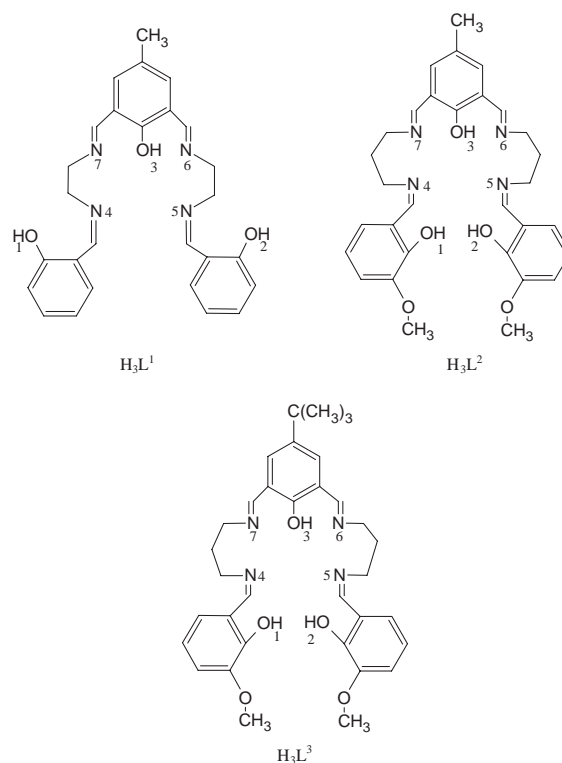
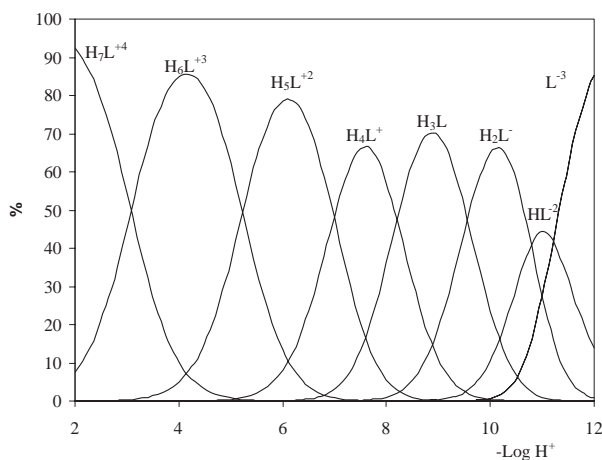Fig. 3. The protonation regions of the Schiff-bases ligands H_3L^1–H_3L^3.

the same protonation constant values. However, when the values in Table 5 are examined, the protonation constants in the related regions are different. The difference in this region can be explained with intermolecular hydrogen bonds.

Potentiometric equilibrium titration curves of the systems consisting of the free ligand H_3L^1 and its Cu(II) and Cd(II) complexes are presented in Fig. 4. The "a" represents the number of moles of base added to the experimental solution per mole of the ligand. In the potentiometric titration curve of the ligand H_3L^1, there are four inflections at $a = 1$, $a = 2$, $a = 3$, and $a = 5$ (where $a = $ moles of base added per mole of ligand). From $a = 0$ to 1, $a = 1$ to 2, $a = 2$ to 3, $a = 3$ to 5, and $a = 5$ to 7, there are three narrow and two extensive buffer regions. The first three narrow buffer regions correspond to the completion of neutralization of the first two most acidic and one neutral ammonium ions. In extensive buffer regions, the other ammonium group and phenolic groups are neutralized. The buffer regions at higher pH are related to the association of the ammonium and phenolic groups in the sequential overlapping steps.
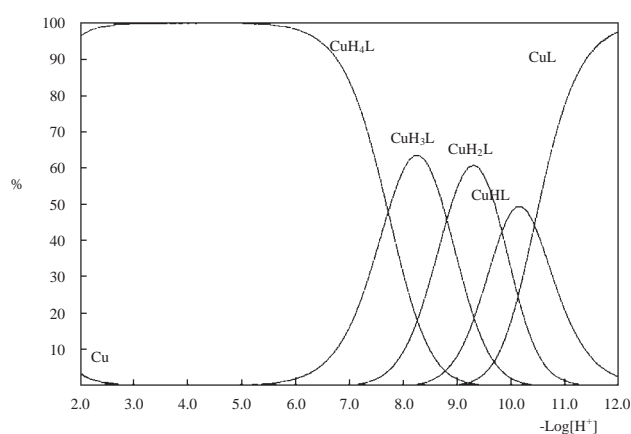
This is also illustrated in the species distribution of the ligand H_3L^1 in Fig. 5. At pH < 4, the ligand exists in the fully protonated form as H_7L^{4+}. As the pH increases, the ligand loses its protons from the imine nitrogens in order to form the

Table 5. Logarithms of the Stability Constants of the Complexes Cu(II) of the Schiff Bases, in 50% Dioxane–Water Mixture ($\mu = 0.100\,\text{M}$ NaClO$_4$, $25.00 \pm 0.02\,^{\circ}$C)

Equilibrium quotient	[Cu$_2$(L^1)Cl]Cl	[Cu$_2$(L^2)Cl]Cl	[Cu$_2$(L^3)Cl]Cl	[Cd$_2$(L^1)Cl]Cl	[Cd$_2$(L^2)Cl]Cl	[Cd$_2$(L^3)Cl]Cl
	Log β	Log β	Log β	Log β	Log β	Log β
[H$_4$ML]/[M][L][H]^4	54.78 ± 0.04	55.65 ± 0.04	55.57 ± 0.06	49.5 ± 0.1	49.03 ± 0.09	48.95 ± 0.10
[H$_3$ML]/[M][L][H]^3	47.06 ± 0.04	47.46 ± 0.03	47.43 ± 0.05	42.28 ± 0.08	42.50 ± 0.07	42.41 ± 0.08
[H$_2$ML]/[M][L][H]^2	38.25 ± 0.03	38.50 ± 0.03	38.41 ± 0.04	34.63 ± 0.08	34.67 ± 0.07	34.54 ± 0.08
[HML]/[M][L][H]	28.42 ± 0.03	28.25 ± 0.02	28.31 ± 0.04	25.68 ± 0.06	25.73 ± 0.05	25.58 ± 0.07
[ML]/[M][L]	17.99 ± 0.02	17.80 ± 0.02	17.75 ± 0.03	15.71 ± 0.06	15.75 ± 0.04	15.61 ± 0.07
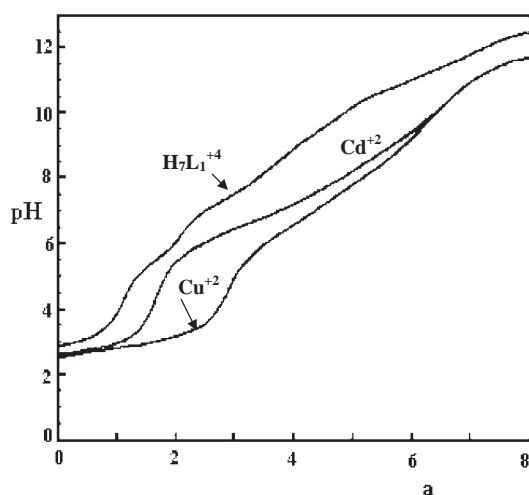
Fig. 4. Potentiometric titration curves for the Schiff base H$_3$L^1 and 1:1 stoichiometries of Cu(II) and Cd(II) to the Schiff base H$_3$L^1 (ML) as a function of added NaOH (a = moles of base added per mole of metal ion (or ligand)).

Fig. 6. Species distribution diagram for the Cu–L^1 Schiff-base system in 1:1 molar ratio as a function of the pH. $\mu = 0.100\,\text{M}$ NaClO$_4$, $t = 25.0\,^{\circ}$C, $T_L = 1.5 \times 10^{-3}$ M, $T_{Cu} = 1.5 \times 10^{-3}$ M, % = percentage concentration of species.

Fig. 5. Species distribution diagram for the Schiff-base (H$_3$L^1) systems as a function of the pH. $\mu = 0.100\,\text{M}$ NaClO$_4$, $t = 25.0\,^{\circ}$C, $T_L = 1.5 \times 10^{-3}$ M, % = percentage concentration of species.

H$_6$L^{3+}, H$_5$L^{2+}, and H$_4$L$^+$ species, respectively. H$_6$L^{3+} is the predominant species in the pH range 2–7 and its maximum concentration reaches 85.5% at pH = 4.2. When the pH is above 6, one of the three phenolic hydroxy protons begins to deprotonated to form H$_3$L, which reaches its maximum concentration (72.0%) at pH = 9.0. The log values of overall pro-

tonation constant, log β^H, for the Schiff base H$_3$L^2 is 55.61, whereas for the corresponding smaller Schiff base H$_3$L^3 containing the *t*-butyl group is 54.88. Thus, the Schiff base H$_3$L^2 displays a much stronger overall basic character than the ligand H$_3$L^3. These results can be explained in that the *t*-butyl group in H$_3$L^3 Schiff base gives more electron density than the ligand H$_3$L^2 with the inductive effect.

Stability Constants of the Schiff-Bases Complexes. The potentiometric titration curves of the ligand H$_3$L^1 with equivalents of ligand to metal ion for Cd(II) and Cu(II) are shown in Fig. 6. The metal ions depress the titration curve of the free ligand by the release of protons according to the abilities of the metal ions to bind to the ligand Schiff bases. As the titration curves of the complexes formed by cadmium and copper together with the Schiff base H$_3$L^1 are examined, two inflection points can be observed at $a = 2$ and $a = 6$ for Cd(II), and at $a = 3$ and $a = 6$ for Cu(II). The presence of an inflection point on the titration curves at $a = 3$ and $a = 2$ for the Cu(II) and Cd(II), respectively, can be explained by the formation of protonated complexes. The ligand H$_3$L^1, because of its geometric shape, can not form bonds with the metal ion at every protonation region; as a result, the protonated complexes are formed in an acidic medium. For example, the oxygen atoms of the basic phonolate anion and one of the nitrogen atoms of the imine group are protonated in the Cu–L^1 system and the CuH$_4$L complex forms, and oxygens of the phonolate anion and two of the nitrogen atoms of the imine group are protonated in the Cd–L^1 system and CdH$_5$L complex forms. The Cu(II)

Table 6. Logarithms of the Stability Constants of the Complexes Cd(II) of the Schiff Bases, in 50% Dioxane–Water Mixture ($\mu = 0.100$ M NaClO$_4$, $t = 25.00 \pm 0.02\,^\circ$C)

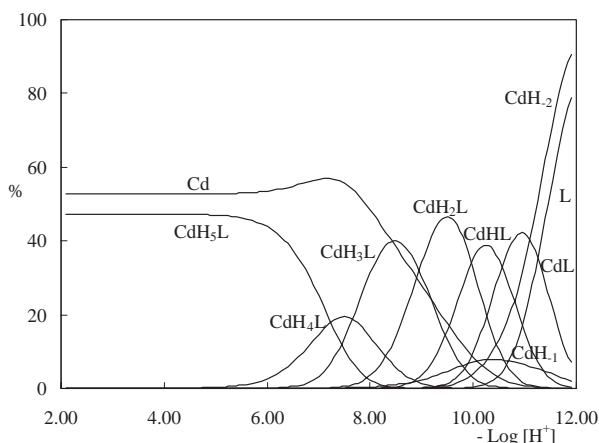| Equilibrium quotient	H_3L^1	H_3L^2	H_3L^3
	Log β	Log β	Log β
$[H_5ML]/[M][L][H]^5$	49.5 ± 0.1	49.03 ± 0.09	48.95 ± 0.10
$[H_4ML]/[M][L][H]^4$	42.28 ± 0.08	42.50 ± 0.07	42.41 ± 0.08
$[H_3ML]/[M][L][H]^3$	34.63 ± 0.08	34.67 ± 0.07	34.54 ± 0.08
$[H_2ML]/[M][L][H]^2$	25.68 ± 0.06	25.73 ± 0.05	25.58 ± 0.07
$[HML]/[M][L][H]$	15.71 ± 0.06	15.75 ± 0.04	15.61 ± 0.07
$[ML]/[M][L]$	5.15 ± 0.04	5.11 ± 0.03	5.07 ± 0.05

Fig. 7. Species distribution diagram for the Cd–L^1 Schiff-base system in 1:1 molar ratio as a function of the pH. $\mu = 0.100$ M NaClO$_4$, $t = 25.0\,^\circ$C, $T_L = 1.5 \times 10^{-3}$ M, $T_{Cd} = 1.5 \times 10^{-3}$ M, % = percentage concentration of species.

ion, which is known to form complexes of tetragonal shape, does not show an inflection point at $a = 4$; this is because a proton is removed from the protonated complex and the protonation constants of the ligand intersects each other.

The stoichiometric stability constants of the metal complexes (Cu(II) and Cd(II)) of the investigated Schiff bases were determined in the 50% dioxane–water mixture at 25 °C and these constants are given in Tables 5 and 6. The metal ions Cu(II) and Cd(II) were found to combine easily with the Schiff bases H_3L^1, H_3L^2, and H_3L^3 to form deprotonated (ML) and multiprotonated (MH$_n$L) in concentrations depending on the pH value of the solution. When the values in Tables 5 and 6 are examined, the following row is obtained for stability constants of the mononuclear complexes (ML) of the Schiff bases: $H_3L^1 > H_3L^2 > H_3L^3$. When these rows, which are obtained for stability constants of the Schiff bases, are compared with the row that is obtained for protonation constants, it is seen that there is no correlation between the stability constants and protonation constants. The order of the stability constants for all ligands was found to be Cu(II) > Cd(II), in agreement with the increasing acidity of the metal ion. Comparison of the Cu(II) and Cd(II) complexes of these three ligands indicate that the size of the cavity in the ligands and metal ion radius plays an important factor in the stability of mononuclear complex formation.[29,31] The cavity is too small to allow complex-

ation of the cadmium ion (Cd(II)) (its radius is larger than the Cu(II) ion). Therefore, the stability constants of the Cd(II) complexes are much smaller than the stability constants of the Cu(II) complexes.

The species distribution curve of the Cd–L^1 system is very different from the Cu–L^1 system because the hydrolysis of cadmium is more dominant than the formation of Cd–L^1 complexes. In the Cd–L^1 system, the complex CdH$_2$L is the most predominate species (Fig. 7) and its maximum, 46.6%, is reached at pH = 9.5. The next most predominate species are the complexes CdH$_5$L, CdH$_3$L, CdHL, and CdL. These complexes have almost the same percentages. The percentage of the species CdH$_4$L is the smallest in this system.

Supporting Information

Supplementary data associated with this article can be found in the online version of this journal. This material is available free of charge on the web at http://www.csj.jp/journals/bcsj/.

References

1   E. Hadjoudis, *Mol. Eng.* **1995**, *5*, 301.

2   T. Dziembowska, *Pol. J. Chem.* **1998**, *72*, 193.

3   A. Filarowski, T. Glowiak, A. Koll, *J. Mol. Struct.* **1995**, *484*, 75.

4   T. Sekikawa, T. Kobayashi, T. Inabe, *J. Phys. Chem. A* **1997**, *101*, 644.

5   B. Zheng, S. Brett, J. P. Tite, T. A. Brodie, J. Rhodes, *Science* **1992**, *256*, 1560.

6   E. Kılıç, F. Köseoğlu, E. Canel, *Indian J. Chem.* **1997**, *36*, 115.

7   G. S. Patterson, R. H. Holm, *Bioinorg. Chem.* **1975**, *4*, 257.

8   D. B. Rorabacher, M. J. Martin, M. J. Koenigbauer, M. Malik, P. R. Schroeder, J. F. Eudicott, L. A. Ochrymowyez, in *Copper Coordination Chemistry: Biochemical and Inorganic Perspectives*, ed. by K. D. Karlin, J. Zubieta, Academic Press, New York, **1983**.

9   A. E. Martell, R. J. Motekaitis, *The Determination and Use of Stability Constants*, VCH, New York, **1988**.

10   D. D. Perrin, W. L. F. Armarego, *Purification of Laboratory Chemicals*, Pergamon, **1992**.

11   G. Schwarzenbach, M. Flascha, *Complexometric Titrations*, Methuen, London, **1957**.

12   F. J. C. Rossotti, H. Rossotti, *J. Chem. Educ.* **1965**, *7*, 375.

13   G. Gran, *Acta Chem. Scand.* **1950**, *4*, 559.

14   T. N. Sorrell, C. O'Connor, O. P. Anderson, J. H. Reibenspies, *J. Am. Chem. Soc.* **1985**, *107*, 4199.

15   H. Rossotti, *The Study of Ionic Equilibria: An Introduction*, Longman, London, **1978**.

16   P. May, D. R. Williams, P. W. Linder, R. G. Torrington, *Talanta* **1982**, *29*, 249.

17   P. Serjant, *Potentiometry and Potentiometric Titrations*, Wiley, New York, **1984**.

18   D. M. Boghaci, M. Lashanizadegan, *J. Sci., Islamic Repub. Iran* **2000**, *11*, 301.

19   D. M. Boghaci, M. Lashanizadegan, *Synth. React. Inorg. Met.-Org. Chem.* **2000**, *30*, 1535.

20   D. Cunningham, P. McArdle, M. Mitchell, N. N. Chonchubhair, M. O'Gara, F. Franceschi, C. Floriani, *Inorg. Chem.* **2000**, *39*, 1639.

21   M. Tümer, C. Çelik, H. Köksal, S. Serin, *Transition Met. Chem.* **1999**, *24*, 525.

22 a) M. Tümer, H. Köksal, S. Serin, M. Dığrak, *Transition Met. Chem.* **1999**, *24*, 13. b) A. Gölcü, M. Tümer, H. Demirelli, R. A. Wheatley, *Inorg. Chim. Acta* **2005**, *358*, 1785.

23 H. Köksal, M. Dolaz, M. Tümer, S. Serin, *Synth. React. Inorg. Met.-Org. Chem.* **2001**, *31*, 1141.

24 R. Atkins, G. Brewer, E. Kokot, G. M. Mockler, E. Sinn, *Inorg. Chem.* **1985**, *24*, 127.

25 A. L. Nivorozhkin, H. Toflund, P. L. Jorgensen, L. E. Nivorozhkin, *J. Chem. Soc., Dalton Trans.* **1996**, 1215.

26 W. J. Geary, *Coord. Chem. Rev.* **1971**, *7*, 81.

27 a) M. Dolaz, M. Tümer, *Transition Met. Chem.* **2004**, *29*, 516. b) J. Mukherjee, R. Gupta, T. Mallah, R. Mukherjee, *Inorg. Chim. Acta* **2005**, *358*, 2711.

28 M. Dolaz, M. Tümer, M. Dığrak, *Transition Met. Chem.* **2004**, *29*, 528.

29 D. Kong, J. Mao, A. E. Martell, A. Clearfield, *Inorg. Chim. Acta* **2002**, *338*, 78.

30 G. Shangguan, A. E. Martell, Z. Zhang, J. H. Reibenspies, *Inorg. Chim. Acta* **2000**, *299*, 47.

31 A. E. Martell, R. D. Hancock, *Metal Complexes in Aqueous Solutions*, Plenum Press, New York, **1996**.